DOI: 10.2478/auoc-2025-0017

Ovidius University Annals of Chemistry Volume 35, Issue 1, pp. 143 - 148, 2025

Sodium chloride-activated rubber seed shell carbon for methylene blue removal

Kah Yee CHOOI,[1] Fadina AMRAN,[1] and Muhammad Abbas AHMAD-ZAINI[*1,2]

[1]*Faculty of Chemical & Energy Engineering, Universiti Teknologi Malaysia, 81310 UTM Johor Bahru, Johor, Malaysia*

[2]*Centre of Lipids Engineering & Applied Research (CLEAR), Ibnu-Sina Institute for Scientific & Industrial Research (ISI-SIR), Universiti Teknologi Malaysia, 81310 UTM Johor Bahru, Johor, Malaysia*

Abstract. Rubber seed shell was converted into adsorbents via sodium chloride activation at mass ratios (NaCl-to-rubber seed shell) of 0.5, 1.0, and 2.0 for methylene blue adsorption. The char (without NaCl activation) was also prepared for comparison. The adsorbents were characterized for specific area, functional groups, and morphology, while the dye adsorption was studied at different concentrations, contact times, and solution temperatures for equilibrium, kinetics, and thermodynamics, respectively. The surface morphology of activated carbon becomes more porous when NaCl concentration for activation increases. The textural analysis shows a greater specific area of 330 m^2/g for activated carbon by NaCl activation at a mass ratio of 0.5, while char exhibits the magnitude of only 68.8 m^2/g. However, the latter exhibits the best adsorptive performance for methylene blue. The char displays a greater pore size of 4.7 nm, while all activated carbons are relatively microporous, thus inhibiting the smooth diffusion of dye molecules.

***Keywords*:** activated carbon; adsorption; rubber seed shell; NaCl activation; methylene blue.

1. Introduction

Textile industry is one of the largest chemical industries in the world; it significantly contributes to the economic growth. The global production of dyes is nearly 8×10^5 tons per year. However, synthetic dyes may eventually leak from the process and find their way into streams, so polluting the ecosystem [1]. About 10-15 % of dyes is lost during different processes in the textile industry. Over the time, dyes accumulate in the water, to such an extent that light can no longer penetrate into the surface which impairs the ability of aquatic plants to perform photosynthesis, leading to an increase in oxygen demand. Besides, some dyes are carcinogenic which can cause cancer [2]. Long exposure to dye-contaminated water can cause skin irritation and other health issues. Consequently, the effluent discharge from textile industries without sufficient treatment will bring negative implications to the environment and human health [1].

Various methods have been developed for dye removal, including coagulation and flocculation, membrane filtration, adsorption, chemical oxidation, advanced oxidation processes and photodegradation. Among others, adsorption is considered a preferred method for dye removal because of its cost-competitiveness and high performance, attributed to the large surface area and strong affinity of adsorbents for dye molecules. Moreover, bio-based adsorbents are more advantageous than chemically synthesized ones due to their lower toxicity, renewability, cheapness, and straightforward preparation steps [3].

The adsorbent feedstock used in this study is rubber seed shell (RSS). RSS is an abundantly available resource from rubber plantation. According to the Malaysia Natural Rubber Industry (MNRI), the natural rubber production in 2019 is 61,731 tons from 1.1 million hectares of plantations. Meanwhile, biomass residues such as RSS remain largely underutilized, despite their potential as low-cost adsorbents [4]. About 1000 kg of RSS per hectare per year is expected to be generated from the plantation sector [4, 5]. So, it offers a sustainable feedstock for adsorbent and supports the advancement of zero-waste production. RSS contains high percentage of carbon of 49.5 %, making it a suitable precursor for activated carbon production [5]. Also, it has low ash content of 0.2 %. A high ash content can interfere the activation process and reduce the quality of resultant activated carbon [5]. The hard texture of RSS allows it to decorate the porous structure during activation that often results in high surface area of activated carbon [4].

The novelty of this work lies on the use of sodium chloride (NaCl) to activate RSS. NaCl is a less toxic activator with insignificant impacts on the environment. Three NaCl-to-rubber seed shell mass ratios were employed, and the activated carbons were used for the removal of methylene blue. NaCl is a promising activator to decorate the porous structure that brings about sufficient surface area of activated carbons. Finally, the activated carbons were characterized and the adsorption data were analyzed and discussed.

2. Experimental

2.1. Materials

Rubber seed shell (RSS) was collected from a local rubber plantation in Johor state of Malaysia. Sodium

* Corresponding author. *E-mail address*: abbas@cheme.utm.my (Muhammad Abbas Ahmad Zaini).

chloride (NaCl) and methylene blue (CI 52015) were supplied by R&M Chemicals (Malaysia). NaCl was used for the activation of rubber seed shell, while methylene blue ($C_{16}H_{18}N_3SCl$) with molecular weight 319.85 g/mol was used to produce synthetic dye wastewater for adsorption tests.

2.2. Methods

RSS was washed with water to remove surface impurities and dried in an oven at 110 °C for 24 h. Next, it was crushed to a uniform size of 5 mm. A 2.5 g NaCl was mixed with 5 g RSS (NaCl-to-RSS ratio of 0.5). NaCl was dissolved in distilled water and the mixture was stirred on a hot plate at 80 °C for 20 min and oven-dried overnight for impregnation. After that, the impregnated sample was transferred into a crucible and covered with aluminum foil. The activation was performed in a furnace at 550 °C for 1 h. The resultant activated carbon was washed with hot distilled water, dried and stored prior to use.

Similar steps were repeated for NaCl activation at mass ratios of 1:1 (5 g NaCl) and 2:1 (10 g NaCl). The RSS char (without NaCl) was also prepared for comparison. The char and activated carbons prepared at mass ratios 0.5, 1.0, and 2.0 were designated as samples A, B, C and D, respectively. The yield of activated carbon was determined as [6]:

$$Yield, \% = \frac{W_{AC}}{W_o} \times 100 \qquad (1)$$

where W_{AC} = dry weight of activated carbon (g) and W_o = initial weight of RSS (g).

The activated carbons were characterized for textural properties by N_2 gas adsorption at 77 K using a BET Micromeritics TriStar II 3020. The surface morphology was obtained by a scanning electron microscope (SEM) TM3000 (Hitachi Japan). The FTIR spectra were determined using an infrared spectrometer Spectrum One (Perkin Elmer, USA).

The effect of concentration on dye adsorption was performed by adding 30 mg of adsorbent into 30 mL of dye solution at different concentrations of 5 to 200 mg/L. A control solution without adsorbent was prepared to represent initial concentration. The mixture was allowed to reach equilibrium for 72 h, and the concentration was measured using a visible spectrophotometer Spectrumlab 750Pro at wavelength of 600 nm. The dye adsorption capacity at equilibrium, Q_e was calculated as [4]:

$$Q_e = \frac{(C_0 - C_e)}{m} V \qquad (2)$$

where C_e and C_0 (mg/L) are the equilibrium and initial concentrations of dye, respectively, m (g) is the mass of adsorbent, and V (L) is the solution volume. The adsorption data were analyzed using Langmuir and Freundlich models [4]:

$$Q_e = \frac{Q_m \cdot b \cdot C_e}{1 + b \cdot C_e} \qquad (3)$$

$$Q_e = K_F C_e^{1/n} \qquad (4)$$

where, Q_m (mg/g) is the maximum adsorption capacity, b (L/mg) is the Langmuir constant, K_F (mg/g)·(L/mg)$^{1/n}$ is the Freundlich capacity, and n is the adsorption intensity.

For the effect of contact time on dye adsorption, the residual concentration was measured using a visible spectrophotometer at pre-set intervals from 5 min until the equilibrium is attained. The concentration of methylene blue was fixed at 10 mg/L, and additional concentrations of 5 mg/L and 20 mg/L were introduced to assess the kinetics of adsorbent with greater methylene blue capacity. The adsorption capacity at time t, Q_t was calculated as [5]:

$$Q_t = \frac{(C_0 - C_t)}{m} V \qquad (5)$$

where C_t (mg/L) is the concentration of dye at time t. The kinetics data were analyzed using pseudo-first-order and pseudo-second-order models [4]:

$$Q_t = Q_e(1 - e^{-k_1 t}) \qquad (6)$$

$$Q_t = \frac{Q_e^2 k_2 t}{1 + Q_e k_2 t} \qquad (7)$$

where k_1 (1/min) and k_2 (g/mg·min) are the pseudo-first-order and pseudo-second-order rate constants. All models were solved by non-linear regression using Solver of MS Excel by minimizing the sum-of-squared errors (SSE) to optimize the regression coefficient (R^2).

The effect of temperature on dye adsorption was conducted in a temperature-regulated water bath at solution temperatures of 40 °C, 50 °C, and 60 °C. The methylene blue concentration was fixed at 20 mg/L. The residual concentration was measured using a visible spectrophotometer after 72 h. The thermodynamic parameters of Gibbs free energy ($\Delta G°$), entropy ($\Delta S°$) and enthalpy ($\Delta H°$) were determined from [3]:

$$\ln(K_d) = -\frac{\Delta H}{RT} + \frac{\Delta S}{R} \qquad (8)$$

$$\Delta G = -RT \ln(K_d) \qquad (9)$$

$$K_d = \frac{Q_e}{C_e} \qquad (10)$$

where K_d is the equilibrium constant, and $\Delta H°$ and $\Delta S°$ were calculated from the slope and y-intercept of the linear plot of ln K_d against 1/T.

3. Results and discussion

3.1. Characteristics of adsorbents

Table 1 summarizes the characteristics of adsorbents, i.e., char (A) and RSS activated carbons by NaCl activation at mass ratios of 0.5 (B), 1.0 (C) and 2.0 (C). The yield of adsorbents decreased with increasing mass ratio of NaCl-to-RSS. The presence of NaCl within the RSS matrix encourages the evolution of volatiles and carbon burning-off during the activation at high temperature [7, 8].

Table 1. The characteristics of adsorbents

Adsorbent sample	A	B	C	D
Yield (%)	72.3	18.4	12.8	9.71
S_{BET} (m^2/g)	68.8	330	324	317
Total pore volume (cm^3/g)	0.0809	0.198	0.217	0.195

Adsorbent sample	A	B	C	D
Micropore volume (cm^3/g)	0.0446	0.114	0.142	0.106
Mesopore content (%)	44.9	42.4	34.5	45.6
Average pore diameter (nm)	4.70	2.40	2.68	2.46

As the NaCl ratio increases from 0.5 to 2.0, the specific area (S_{BET}) of activated carbons slightly decreased from 330 to 317 m^2/g, while char exhibits the S_{BET} of only 68.8 m^2/g. It shows that NaCl remarkably increases the specific area of an adsorbent upon activation [3]. NaCl acts as a template that enhances the S_{BET} by promoting the surface roughness and formation of micropores. During the carbon burning-off, NaCl also facilitates the development of interconnected pore channels, thereby improving the diffusion of volatiles and carbon porosity [9]. The average pore diameter of activated carbons is in the range of 2.40 to 2.68 nm, while char, despite its low S_{BET}, displays a greater pore diameter of 4.70 nm, implying that all adsorbents are predominantly mesoporous [10].

The adsorptive performance of activated carbon also relies on the chemical reactivity of functional groups on its surface. Figure 1 shows the FTIR spectra of all adsorbents. All samples depict a broad band at 3700-3200 cm^{-1}, ascribed to O–H stretching of hydroxyl groups and moisture in the cellulose material [6].

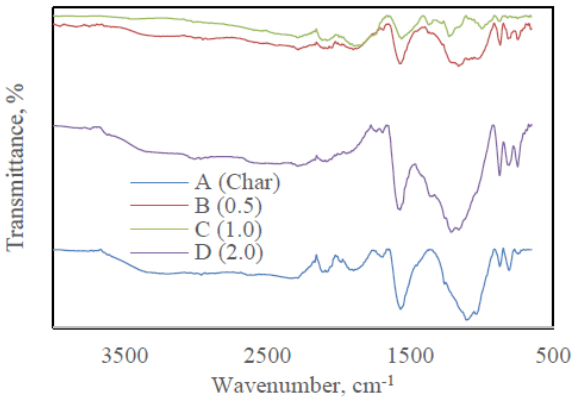

Figure 1. FTIR spectra of adsorbents

A sharp peak at 1570-1562 cm^{-1} corresponds to the C=C bonds. A low intensity peak at 2970-2950 cm^{-1} belongs to C–H stretching vibrations, associated with aliphatic $–CH_2$ and $–CH_3$ groups. For activated carbon samples, the intensity is mild, implying the transformation of aliphatic chains into graphitic structure with some liberation of volatiles during NaCl activation. The peak at 1690 cm^{-1} is attributed to C=O stretching of carboxyl groups in activated carbons. In addition, all activated carbon samples exhibit a peak at 1228-1160 cm^{-1}, indicating C–O stretching vibrations originating from the lignocellulosic components in RSS [4, 6].

The SEM was used to observe the physical morphology of the prepared samples [11]. Figure 2 displays the SEM images of adsorbents. The surface of activated carbons is smooth with considerable number of pore openings, suggesting the high S_{BET} of the materials [12]. As the NaCl concentration increases, the pore development is uniformly distributed over the surface. Conversely, char establishes a rough structure with insignificant pore development on its surface. The NaCl activation promotes the development of pore volume as a result of its reaction with lignocellulosic material [11, 13]. However, excessive amount of NaCl may lead to destruction of porous structure.

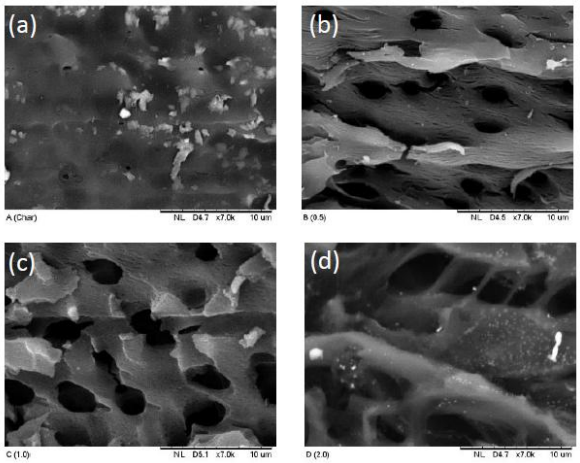

Figure 2. SEM images of adsorbents, (a) A: char, and NaCl activated carbons at ratios of (b) 0.5, (c) 1.0, and (d) 2.0.

3.2. Equilibrium adsorption

The effect of methylene blue concentration was carried out to determine the maximum loading of dye onto adsorbents. The equilibrium adsorption is essential in upscaling the process in practical operation. Figure 3 shows the equilibrium of methylene blue adsorption by adsorbents.

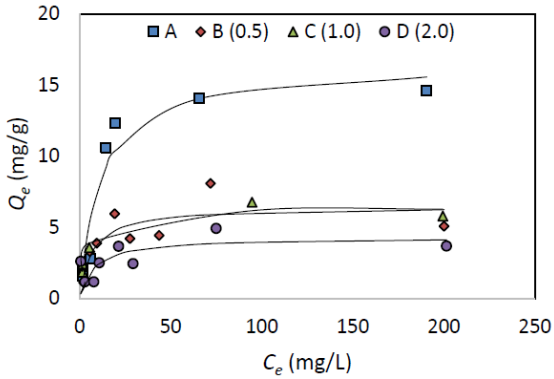

Figure 3. The equilibrium of methylene blue adsorption onto adsorbents (lines were fitted using Langmuir model)

From Figure 3, the char (sample A) demonstrates a greater removal of methylene blue. The maximum capacity was recorded at 14.6 mg/g. Samples B and C display a comparable performance of 6.30 mg/g, while sample D exhibits a poor removal of only 4.14 mg/g. Although the S_{BET} of activated carbons is greater than that of the char, their textural characteristics offer trivial impact towards dye adsorption. A greater performance of char can be ascribed to its larger average pore diameter. Char with pore diameter of 4.70 nm allows more dye molecules to diffuse and lodge on its surface, thereby increasing the adsorption capacity [14]. Conversely, the smaller pore diameter of activated carbons restricts the diffusion of dye molecules. Also, the deposition of Na cations on the carbon surface could

possibly repulse the incoming positively charge dye molecules in the solution, so decreasing the removal capacity [15].

Table 2 summarizes the constants of Langmuir and Freundlich isotherm models.

Table 2. The constants of isotherm models

Sample	A	B	C	D
$Q_{,exp}$ (mg/g)	14.6	6.30	6.30	4.14
Langmuir				
Q_m (mg/g)	16.5	6.47	6.41	4.31
b (L/mg)	0.0867	0.145	0.291	0.121
R^2	0.927	0.723	0.956	0.440
SSE	15.8	10.7	0.790	8.38
Freundlich				
K_F (mg/g) (L/mg)	3.49	2.13	2.31	1.63
$1/n$	0.300	0.223	0.199	0.183
R^2	0.758	0.532	0.870	0.448
SSE	51.6	18.1	2.34	6.39

The equilibrium data fitted best into Langmuir model with reasonably higher R^2 and lower SSE. Except for sample D that exhibits a lower R^2 of 0.440 because the data are scattered at smaller Q_e values. Accordingly, the adsorption can be described as monolayer coverage onto homogeneous carbon surface [16]. The values of the maximum adsorption capacity (Q_m) show close agreement with the experimental data, signifying the accuracy of the model to predict the capacity at equilibrium.

3.3. Adsorption kinetics

Adsorption kinetics describe the rate of methylene blue removal by adsorbents and the time required to reach equilibrium. Figure 4 shows the rate of methylene blue adsorption onto adsorbents. The dye capacity for char increased with increasing concentration, but the time needed to attain equilibrium becomes longer [17]. The adsorbents took around 2-3 days to reach equilibrium.

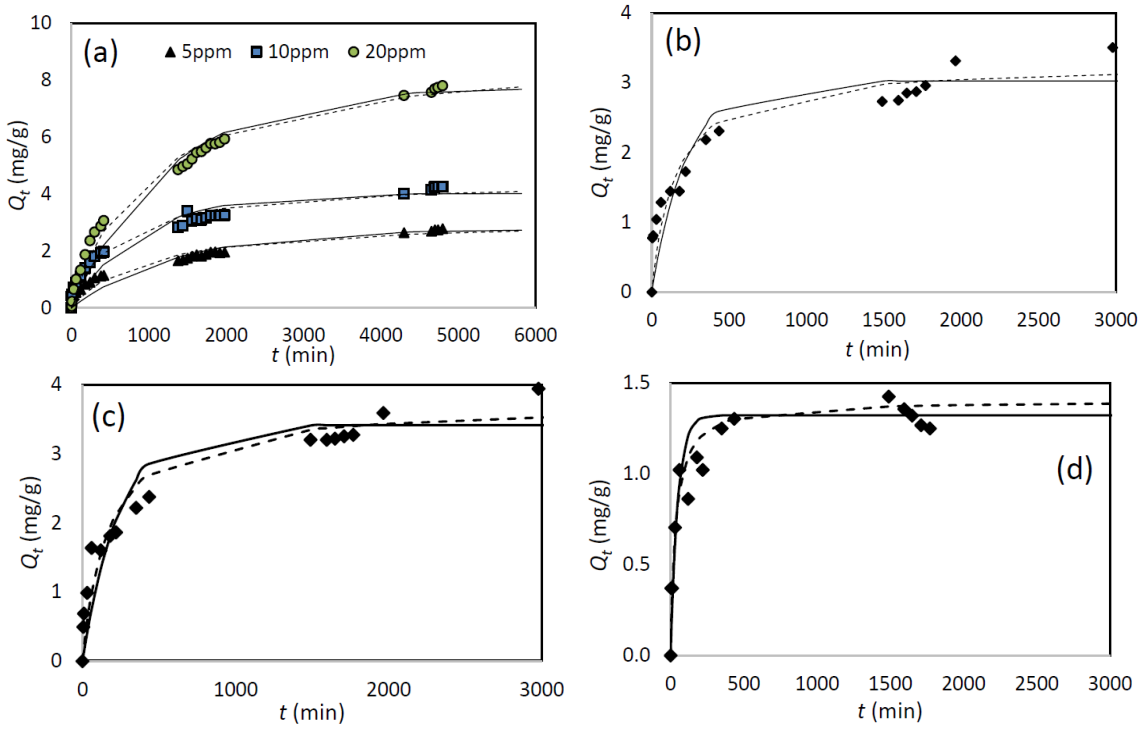

Figure 4. The rate of methylene blue adsorption by (a) char at different concentrations, and NaCl activated carbons by ratios of (b) 0.5, (c) 1.0, and (d) 2.0 at C_o = 10 mg/L (solid lines: pseudo-first order model; dashed lines: pseudo-second order model).

Table 3. The constants of kinetic models

Sample		A		B	C	D
C_o (mg/L)	5.0	10	20	10	10	10
$Q_{,exp}$ (mg/g)	2.62	4.02	7.80	3.31	3.38	1.37
Pseudo-first order						
Q_e (mg/g)	2.77	4.02	7.75	3.03	3.42	1.32
k_1 (min^{-1})	7.0×10^{-4}	1.10 ×10^{-3}	8.0×10^{-4}	4.5×10^{-3}	4.1×10^{-3}	2.1×10^{-2}
SSE	1.93	4.83	6.36	2.76	2.95	0.541
R^2	0.96	0.96	0.98	0.91	0.92	0.86
Pseudo-second order						
Q_e (mg/g)	3.14	4.49	9.10	3.28	3.72	1.40
k_2 (g/mg. min)	3.0×10^{-4}	4.0×10^{-4}	1.0×10^{-4}	2.0×10^{-3}	1.6×10^{-3}	2.1×10^{-2}
SSE	1.26	2.34	2.89	1.93	1.80	0.293
R^2	0.97	0.97	0.99	0.93	0.95	0.92

Table 3 summarizes the constants of kinetic models. The kinetics data fitted well into pseudo-second order model with higher R^2 and lower SSE. The model adequately predicts the Q_e values that are closely aligned with the experimental data. The applicability of this model to describe the kinetics data implies that the adsorption rate is controlled by chemisorption [12].

3.4. Adsorption thermodynamics

Figure 5 shows the van't Hoff plot for methylene blue adsorption at different temperatures, and the thermodynamic parameters are summarized in Table 4. The positive $\Delta H°$ (48.8 kJ/mol) indicates that the adsorption by char (sample A) is endothermic, whereby the removal of methylene blue increased with solution temperature. At higher temperature, the viscosity of the solution decreases that brings about an increase in kinetic energy and diffusion rate of dye molecules onto

the active sites. Additionally, the value of $\Delta H°$ > 40 kJ/mol, implying that the process is more driven by chemisorption [16].

The positive $\Delta S°$ (0.154 kJ/mol·K) explains the randomness of the system at the adsorbent-liquid interface during adsorption, with possible structural changes between dye molecules and the adsorbent surface [12]. The negative $\Delta G°$ at 50 °C and 60 °C as recorded by char suggests a removal process that is more spontaneous and favorable with increasing solution temperature [18]. On the contrary, the two activated carbons (samples B and C) show an opposite thermodynamic behavior of adsorption. The adsorption is exothermic and becomes non-spontaneous with increasing solution temperature.

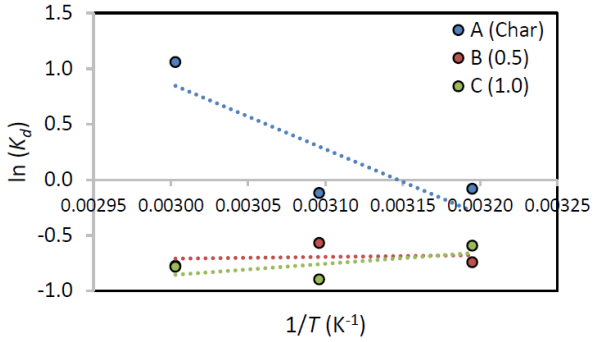

Figure 5. The van't Hoff plot for dye adsorption at different solution temperatures

Table 4. Thermodynamic parameters for methylene blue adsorption onto adsorbents

Sample	*T* (K)	$\Delta H°$ (kJ/mol)	$\Delta S°$ (kJ/mol.K)	$\Delta G°$ (kJ/mol)
A	313	48.8	0.154	0.735
	323			-0.802
	333			-2.34
B	313	-1.30	-9.81×10^{-3}	1.77
	323			1.86
	333			1.96
C	313	-8.46	-3.25×10^{-2}	1.71
	323			2.04
	333			2.36

4. Conclusions

Rubber seed shell (RSS) was converted into char (without NaCl activation) and activated carbons. Three NaCl-to-RSS ratios of 0.5, 1.0, and 2.0 were used to convert RSS into activated carbons. The specific area (S_{BET}) of activated carbons is 5 times higher greater than that of char (S_{BET} = 68.8 m^2/g). The average pore diameter of char is 4.70 nm, nearly doubled that of activated carbons, which brings about higher removal of methylene blue. To conclude, sodium chloride is a promising activator that can produce high surface area activated carbon. Nevertheless, more studies would be required to unlock the true potential of NaCl-activated RSS for wastewater treatment.

Acknowledgement

This work is supported by Ministry of Higher Education Malaysia through Fundamental Research Grant Scheme, FRGS/1/2022/STG05/UTM/02/5.

Conflict of interest

Authors declared that they have no conflict of interest.

References

[1]. R. Altohamy, S. Ali, F. Li, K. Okasha, Y. Mahmoud, T. Elsamahy, H. Jiao, Y. Fu, J. Sun, A critical review on the treatment of dye-containing wastewater: Ecotoxicological and health concerns of textile dyes and possible remediation approaches for environmental safety, Ecotoxicology and Environmental Safety 231 (2022) 113160. Doi: 10.1016/j.ecoenv.2021.113160

[2]. A. Riaz, B. Shreedhar, M. Kamboj, S. Natarajan, Methylene blue as an early diagnostic marker for oral precancer and cancer, SpringerPlus 2 (2013) 95. Doi: 10.1186/2193-1801-2-95

[3]. C.A. Igwegbe, O.D. Onukwuli, J.O. Ighalo, P.U. Okoye, Adsorption of cationic dyes on Dacryodes edulis seeds activated carbon modified using phosphoric acid and sodium chloride, Environmental Processes 7 (2020) 1151-1171. Doi: 10.1007/s40710-020-00467-y

[4]. A. Borhan, S. Yusuf, Activation of rubber-seed shell waste by malic acid as potential CO_2 removal: Isotherm and kinetics studies, Materials 13 (2020) 4970. Doi: 10.3390/ma13214970

[5]. N. Mokti, A. Borhan, S.N.A. Zaine, H.F.M. Zaid, Development of rubber seed shell–activated carbon using impregnated pyridinium-based ionic liquid for enhanced CO_2 adsorption, Processes 9 (2021) 1161. Doi: 10.3390/pr9071161

[6]. H. Sawalha, A. Bader, J. Sarsour, M. Al-Jabari, E.R. Rene, Removal of dye (methylene blue) from wastewater using bio-char derived from agricultural residues in Palestine: Performance and isotherm analysis, Processes 10 (2022) 2039. Doi: 10.3390/pr10102039

[7]. J. Fu, J. Zhang, C. Jin, Effects of temperature, oxygen and steam on pore structure characteristics of coconut husk activated carbon powders prepared by one-step rapid pyrolysis activation process, Bioresource Technology 310 (2020) 123413. Doi: 10.1016/j.biortech.2020.123413

[8]. M.M. Alam, M.A. Hossain, M.D. Hossain, M.A.H. Johir, J. Hossen, M.S. Rahman, J.L. Zhou, A.T.M.K. Hasan, A.K. Karmakar, M.B. Ahmed, The potentiality of rice husk-derived activated carbon: From synthesis to application, Processes 8 (2020) 203. Doi: 10.3390/pr8020203

[9]. M. Gayathiri, T. Pulingam, K.T. Lee, K. Sudesh, Activated carbon from biomass waste precursors: Factors affecting production and adsorption mechanism, Chemosphere 294 (2022) 133764. Doi: 10.1016/j.chemosphere.2022.133764

[10]. K. Pattarith, S. Tangtubtim, S. Thupsuri, Adsorption of hexavalent chromium and methylene blue onto the rubber seed shell activated carbon: Isotherm and kinetic studies, Research Square. Posted online on May 2022. Doi: 10.21203/rs.3.rs-1614108/v1

[11]. S. Joshi, K.C. Bishnu, Synthesis and characterization of sugarcane bagasse based activated carbon: Effect of impregnation ratio of $ZnCl_2$, Journal of Nepal Chemical Society 41 (2020) 74-79. Doi: 10.3126/jncs.v41i1.30490

[12]. K.C. Bedin, A.C. Martins, A.L. Cazetta, O. Pezoti, V.C. Almeida, KOH-activated carbon prepared from sucrose spherical carbon: Adsorption equilibrium, kinetic and thermodynamic studies for methylene blue removal, Chemical Engineering Journal 286 (2016) 476-484. Doi: 10.1016/j.cej.2015.10.099

[13]. S.M. Abegunde, K.S. Idowu, O.M. Adejuwon, T. Adeyemi-Adejolu, A review on the influence of chemical modification on the performance of adsorbents, Resources, Environment and Sustainability 1 (2020) 100001. Doi: 10.1016/j.resenv.2020.100001

[14]. L. Chen, T. Ji, L. Mu, Y. Shi, H. Wang, J. Zhu, Pore size dependent molecular adsorption of cationic dye in biomass derived hierarchically porous carbon, Journal of Environmental Management 196 (2017) 168-177. Doi: 10.1016/j.jenvman.2017.03.013

[15]. L. Pioro, R. Duffey, Current and future nuclear power reactors and plants. In Managing Global Warming, T.M. Letcher (Ed.), Academic Press (2019) pp. 117-197. Doi: 10.1016/B978-0-12-814104-5.00004-1

[16]. T.C. Egbosiuba, A.S. Abdulkareem, A.S. Kovo, E.A. Afolabi, J.O. Tijani, M. Auta, W.D. Roos, Ultrasonic enhanced adsorption of methylene blue onto the optimized surface area of activated carbon: Adsorption isotherm, kinetics and thermodynamics, Chemical Engineering Research and Design 153 (2020) 315-336. Doi: 10.1016/j.cherd.2019.10.016

[17]. A.M. Aljeboree, A.N. Alshirifi, A.F. Alkaim, Kinetics and equilibrium study for the adsorption of textile dyes on coconut shell activated carbon, Arabian Journal of Chemistry 10 (2017) 3381-3393. Doi: 10.1016/j.arabjc.2014.01.020

[18]. S.N. Shankar, D.R. Dinakaran, D.K. Chandran, G. Mantha, B. Srinivasan, U.P.N. Kannaian, Adsorption kinetics, equilibrium and thermodynamics of a textile dye V5BN by a natural nanocomplex material: Clinoptilolite, Energy Nexus 10 (2023) 100197. Doi: 10.1016/j.nexus.2023.100197

Received: 07.08.2025
Received in revised form: 30.11.2025
Accepted: 05.12.2025